Chapter 24
Wavelet Packet Based CT Image Denoising Using Bilateral Method and Bayes Shrinkage Rule

Manoj Diwakar and Pardeep Kumar

24.1 Introduction

The reconstruction process of Computed tomography (CT) is a typical task to get the CT images. There are certain processes to reconstruct the CT images. X-rays are transmitted to human body; raw data is collected by detectors over the different directions, and finally radon and inverse radon transform has been performed to reconstruct the CT images. The efficiency of whole process is important task. But due to software, hardware and other transmissions and mathematical problems the noise may appears in CT images. The reason of noise appear in CT image is also depend on the X-rays transmission. If the higher amount of X-rays are transmitted over the human body organs, then the quality of CT images are good but it may not good for affect human body organs. With low amount of CT images, human body organs may safe but noise is degraded to the quality of CT images. Hence, if noise can be suppressed from low dose CT images, it will good for the society.

Various research have been already done to reduce noise from the CT images, still it is a challenging task. To suppress noise from CT images, three major techniques are categorized: Projection based denoising, Iterative based denoising and Post-processing based denoising. In projection based denoising, the CT images are filtered when CT images are reconstructed through projected X-ray beams such as filtering of sinogram using bilateral filtering over the low dose CT images [1–3]. In iterative based denoising, CT images are reconstructed using an iterative approach such as iterative CT image reconstruction using shearlet transform [4, 5]. The major

M. Diwakar
Department of CSE, DIT University, Dehradun, Uttarakhand, India

P. Kumar (✉)
Department of CSE and IT, Jaypee University of Information Technology, Solan, Himachal Pradesh, India

drawback of iterative reconstruction is high cost computation. In post-processing based denoising, CT images are denoised directly after obtained CT reconstructed images through X-ray computed tomography. Various techniques have been proposed to denoised CT images using post-processing methods. In post-processing, CT images are denoised broadly in two domains: spatial and transform domain. In spatial domain, pixels are directly denoised using mathematical optimization and computation. Linear and non-linear methods in spatial domain are very popular to denosied the CT images where non-linear methods are providing good results in compare of linear methods in terms of sharp and smooth images. Non-linear filters such as bilateral and non-local mean (NLM) filters are very helpful to provide edge preserving denoised CT images. Bilateral filter [6] is a non-iterative, local filtering method which provides edge preserved smoothing data but it is dependent on kernel radius. NLM [7] filter provides denoised images in terms of sharp edges based on self-similarity approach. But due to self-similarity concept, the computation cost is high.

In transform domain, wavelet transform is used where images are decomposed into low and high frequency subbands. The noise has a tendency that it affects over the edges or detail parts in most of the cases. Thresholding is one of the popular ways to denoised the images in transform domain. Before thresholding, a threshold value is estimated which helps to denoised the images. Soft and Hard thresholding are two popular methods for thresholding. In hard thresholding, a threshold value is estimated. Below the estimated threshold value, the wavelet coefficients are set as zero and rest of the values will be same. In soft thresholding, below the estimated threshold value, the wavelet coefficients are set as zero same as hard thresholding and rest of the wavelet coefficients are modified by subtracting the estimated threshold value. Both processes are good but soft threholding provides better outcomes in most of the cases [8–10]. VISUShrink [11], SUREShrink [12] and BayesShrink [13] are the popular thresholding methods for image denoising. In most of the cases, BayesShrink provides better outcomes in compare to VISUShrink and SUREShrink [14–18]. In transform domain, wavelet transform is one powerful tools [19–22] but it also has some limitations. To overcome that, many other transforms are used such as, wavelet packet transform, dual-tree complex wavelet transform, curvelet, tetrolet, framelet and so on.

In CT images, every small detail has their own significance and may be used for diagnosis purpose. With this consideration, a method noise concept is included with bilateral filtering. In this paper wavelet packet thresholding is performed so that maximum high frequency coefficients can be collected and thresholded. The main concept of this proposed scheme is to reduce noise and preserve the edges from the noisy CT images. Rest of the paper is organized as: Sect. 24.2 gives a small description of wavelet packet transform and bilateral filter. In Sect. 24.3, a brief description of proposed method has been defined. The result analysis and comparative results are discussed in Sect. 24.4. Finally, conclusions are defined in Sect. 24.5.

24.2   Wavelet Packet Transform

Wavelet transform is one of the major tools in the area of image and signal processing. The best part of wavelet that it divides the information into low and high frequencies. Further decompositions are possible as per the size of images. The extended version of wavelet transform is wavelet packet transform. Wavelet packet gives the information into low and high frequencies. The only difference between discrete wavelet transform (DWT) and wavelet packet transform (WPT) that WPT gives higher information in compare to DWT. WPT decompose both low and high frequency components while DWT decompose only low frequency components.

24.3   Proposed Methodology

CT images are generally corrupted with additive Gaussian noise. Hence noisy CT images are obtained via simulation methods. It can be expressed as:

$$X\,(m,n) = Y\,(m,n) + \eta\,(m,n) \tag{24.1}$$

Where, $\eta(m,n)$ is a noise coefficient, $Y(m,n)$ and $X(m,n)$ are noiseless and noisy images respectively.

The proposed algorithm has been designed using wavelet packet transform (WPT). WPT is using to obtain low and high frequency components. The low frequency components are filtered using Bilateral method. Similarly, high frequency components are denoised using thresholding.

The formulation of bilateral filter [6] is given below:

$$BF\,[I]_{\mathbf{p}} = \frac{1}{K} \sum_{\mathbf{q} \in S} G_{\sigma_{s}}\left(\|\mathbf{p} - \mathbf{q}\|\right)\; G_{\sigma_{r}}\left(|I_{\mathbf{p}} - I_{\mathbf{q}}|\right)\; I_{\mathbf{q}} \tag{24.2}$$

Where, p and q are two different pixels, K is normalization constant, σ_S and σ_r are control the behavior of bilateral filtering.

It has two filter kernels as shown in Eq. (24.2). The first kernel is used to enhance the edges and works as edge stopping function. The other kernel is works as Gaussian filter which is used for suppressing the Gaussian noise.

To denosie high frequency components, Bayes shrinkage function is used. This function is used to suppress the Gaussian noise from CT images. The method used for estimating threshold value is defined via statistical methods.

The threshold λ can be selected as:

$$\lambda = \left(\frac{\sigma_{\eta}^{2}}{\sigma_{Y}} \right) \tag{24.3}$$

Where the noise variance can be estimated using robust median estimation method [15] as follows:

$$\sigma_\eta^2 = \left[\frac{median \ (|X(m,n)|)}{0.6745} \right]^2, \tag{24.4}$$

Where, $X(m,n) \epsilon HH_L$, L represents respective level in wavelet decomposition. The standard deviation of noise less image (σ_Y) can be estimated as:

$$\sigma_Y^2 = \max \left(\sigma_X^2 - \sigma_\eta^2, \quad 0 \right) \tag{24.5}$$

Where, $\sigma_X^2 = \frac{1}{N} \sum_{i=1}^{N} X_i^2$, and N represent patch size of an input image.

The thresholding function can be expressed as:

$$\hat{X} := \begin{cases} 0 & if \ |X| \ \leq \ \lambda \\ sign(X) & (|X| - \lambda) \ if \ |X| \ > \ \lambda \end{cases} \tag{24.6}$$

The proposed method can be expressed with the following major steps:

Step 1: Perform wavelet packet transform on input noisy CT image to obtain low and high frequency subbands.

Step 2: Perform bilateral method on the low frequency subbands using Eq. (24.2).

Step 3: Perform thresholding over high frequency subbands using following steps:

 i. Estimate noise variance using Eq. (24.4)
ii. Apply thresholding on high frequency subbands using Eq. (24.6)

Step 4: Apply inverse WPT to obtain denoised image.

24.4 Experimental Results

In the experimental result evaluation, the proposed method is performed over the various standard CT images. The size of CT images are 512×512 with additive Gaussian noise. Experimental evaluation are tested with five different noise level σ ∈ [10, 15, 20, 25, 30, 35]. The CT images are obtained from public source database (https://eddie.via.cornell.edu/cgibin/datac/logon.cgi) which are shown in Fig. 24.1. There are six test CT images which are recognized here as CT1, CT2, CT3, CT4, CT5 and CT6, respectively. For result analysis, the noisy CT images are obtained with different noise level. In Fig. 24.2, noisy CT images are obtained with noise level 25. To execute proposed method, values of some parameters are used such as patch size is 10×10, σ_S is 1.2 and σ_r is 0.13.

Fig. 24.1 Input test CT image dataset. (**a**) CT 1 image. (**b**) CT 2 image. (**c**) CT 3 image. (**d**) CT 4 image

(a)   (b)

(c)   (d)
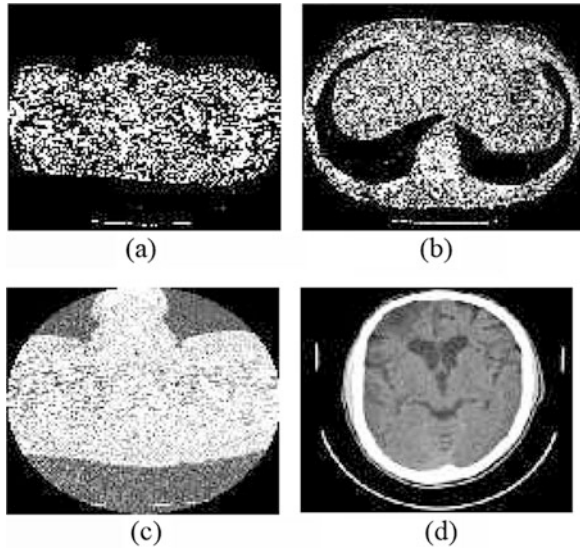
Fig. 24.2 Noisy CT image dataset ($\sigma = 25$). (**a**) CT 1 image. (**b**) CT 2 image. (**c**) CT 3 image. (**d**) CT 4 image

(a)   (b)

(c)   (d)
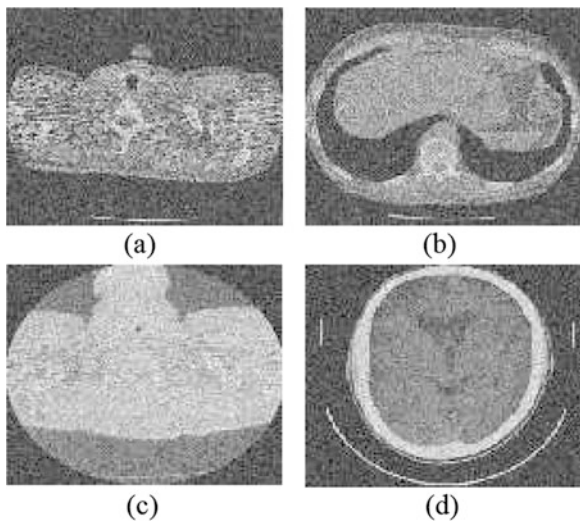
The existing methods for comparison are bilateral filtering [6], Surelet [23] and adaptive wavelet transform with Bayes shrinkage [13]. Figures 24.3, 24.4, 24.5 and 24.6 are showing the results of Bilateral filtering, Surelet, Wavelet based denoising using Bayes shrinkage and proposed method respectively. For comparative study and result analysis, some performance metrics are used to show the performance of methods. The performance metrics which are used, PSNR and IQI.

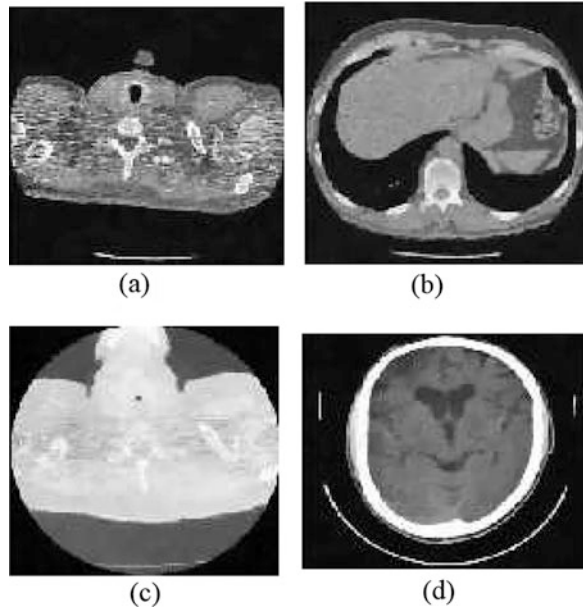**Fig. 24.3** Results of bilateral filtering. (**a**) CT 1 image. (**b**) CT 2 image. (**c**) CT 3 image. (**d**) CT 4 image

(a)

(b)

(c)

(d)

Fig. 24.4 Results of Surelet. (**a**) CT 1 image. (**b**) CT 2 image. (**c**) CT 3 image. (**d**) CT 4 image

(a)

(b)

(c)

(d)
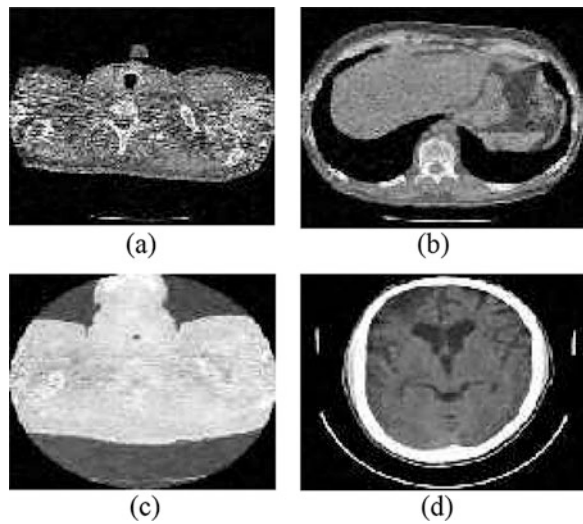
Peak Signal-to-noise Ratio (PSNR) is one major factors to show the performance of methods. Increasing value of PSNR shows that method is good in compare to less PSNR value. The PSNR value can be measured as:

$$PSNR = 10\log_{10}\frac{255^2}{mse} \text{ dB} \qquad (24.7)$$

Fig. 24.5 Results of Bayes
thresholding. (**a**) CT 1 image.
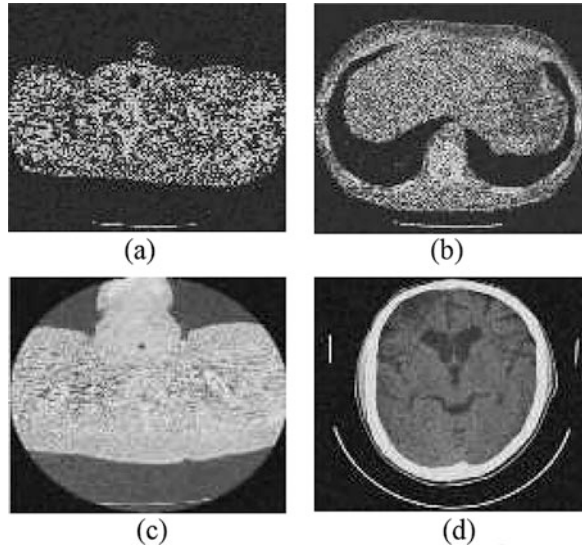(**b**) CT 2 image. (**c**) CT 3
image. (**d**) CT 4 image

(a)   (b)

(c)   (d)

Fig. 24.6 Results of
proposed scheme. (**a**) CT 1
image. (**b**) CT 2 image. (**c**)
CT 3 image. (**d**) CT 4 image

(a)   (b)

(c)   (d)
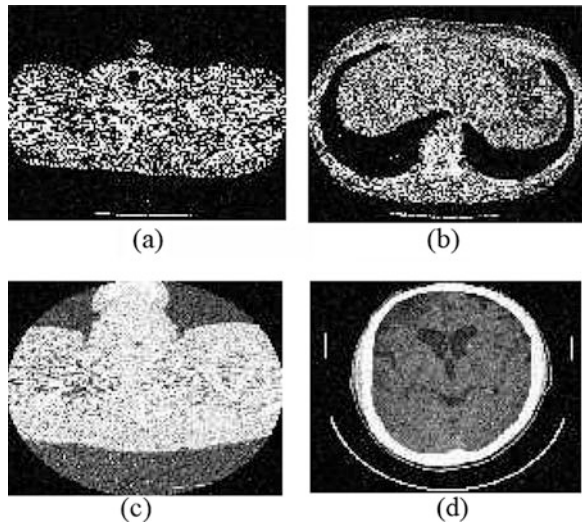
Where $mse = \frac{1}{mn} \sum\limits_{i=1}^{m} \sum\limits_{j=1}^{n} [X(i,j) - W(i,j)]^2$

   Image quality index (IQI) is other important metric which is used to show the results in terms of edge preservation. For input image (X) and denoised image (W), the IQI can be defined as:

$$IQI = \frac{4\sigma_{XW}\overline{X}\overline{W}}{\left(\sigma_X^2 + \sigma_W^2\right)\left[\left(\overline{X}\right)^2 + \left(\overline{W}\right)^2\right]} \qquad (24.8)$$

Where, $\overline{X} = \frac{1}{N}\sum_{i=1}^{N} X_i$, $\overline{W} = \frac{1}{N}\sum_{i=1}^{N} W_i$, $\sigma_X^2 = \frac{1}{N-1}\sum_{i=1}^{N}(X_i - \overline{X})^2$, $\sigma_W^2 =$ $\frac{1}{N-1}\sum_{i=1}^{N}(W_i - \overline{W})^2$ and $\sigma_{XW} = \frac{1}{N-1}\sum_{i=1}^{N}(X_i - \overline{X})(W_i - \overline{W})$.

The results of all existing methods and proposed method indicate that visually, the results of proposed scheme is better in terms of contrast, noise reduction and edge preservation. The values of PSNR and IQI are also indicates that most of the times the results of proposed scheme giving better outcomes.

From Table 24.1, it can be analyzed that proposed method gives minimum value of IQI for different noise level in most of the cases. Similarly, Table 24.2 also indicates that maximum PSNR value is achieved by proposed algorithm in most cases. Hence it can be concluded that proposed algorithm better results in terms noise suppression and edge preservation.

Table 24.1 IQI of denoised images

	σ	TV	Surelet	Bayes	Proposed
CT 1 image	10	0.993	0.9912	0.9924	0.9976
	15	0.9534	0.9856	0.9762	0.9865
	20	0.9312	0.9541	0.9365	0.9597
	25	0.8972	0.9165	0.9174	0.9248
	30	0.8903	0.8954	0.8832	0.8962
	35	0.8894	0.8762	0.8014	0.8747
CT 2 image	0	0.9817	0.9828	0.9751	0.9889
	15	0.9789	0.9794	0.9745	0.9831
	20	0.9421	0.9654	0.9241	0.9521
	25	0.8452	0.8684	0.8922	0.9047
	30	0.8364	0.8361	0.8632	0.8740
	35	0.8189	0.8314	0.8614	0.8694
CT 3 image	10	0.9874	0.9812	0.9914	0.9965
	15	0.9514	0.9614	0.9762	0.9893
	20	0.9423	0.9591	0.9432	0.9614
	25	0.9102	0.9241	0.9397	0.9235
	30	0.8964	0.8931	0.8942	0.9131
	35	0.8831	0.8894	0.8913	0.8941
CT 4 image	10	0.9871	0.9974	0.9954	0.9979
	15	0.9642	0.9831	0.9645	0.9846
	20	0.9409	0.9641	0.9469	0.9698
	25	0.9123	0.9352	0.9231	0.9411
	30	0.8991	0.8978	0.8945	0.9006
	35	0.8647	0.8649	0.8791	0.8771

Table 24.2 PSNR (in dB) of denoised images

	σ	TV	Surelet	Bayes	Proposed
CT 1 image	10	32.14	33.25	31.50	33.9
	15	30.95	31.45	29.96	31.44
	20	29.5	30.10	28.21	30.05
	25	27.98	29.68	28.01	29.85
	30	26.31	28.47	27.25	28.54
	35	25.26	26.19	25.31	26.88
CT 2 image	10	31.54	32.12	30.98	32.47
	15	30.87	30.64	29.42	31.05
	20	28.95	29.08	28.47	29.53
	25	28.48	28.64	27.26	28.96
	30	27.69	28.03	26.17	28.11
	35	25.83	26.96	25.34	26.97
CT 3 image	10	32.33	33.19	31.98	33.89
	15	31.29	31.25	30.67	31.87
	20	29.84	30.98	28.68	30.91
	25	27.15	29.27	28.34	29.31
	30	26.29	28.54	27.52	28.67
	35	24.36	26.65	24.64	26.73
CT 4 image	10	32.65	33.65	31.63	33.79
	15	31.35	31.24	29.26	31.35
	20	29.64	30.19	28.31	30.61
	25	27.45	29.34	28.72	29.36
	30	26.64	28.21	27.37	28.42
	35	25.39	26.94	25.61	26.61

24.5   Conclusions

CT images which are degraded with Gaussian noise are filtered with proposed method and some standard recent existing methods. The utilization of bilateral filter in proposed algorithm gives better results for providing better noise suppression and edge preservation. From results, it was observed that mostly results of proposed scheme are giving better outcomes in terms of noise suppression and edge preservation. The proposed scheme is effectively suppress the noise from CT images as well as also helpful to preserve the edges and structural details.

References

1. A. Manduca, L. Yu, J. D. Trzasko, N. Khaylova, J. M. Kofler, C. M. McCollough and J. G. Fletcher, "Projection space denoising with bilateral filtering and CT noise modeling for dose reduction in CT," International Journal of Medical Physics Research and Practice, Vol. 36, No. 11, pp. 4911–4919, 2009.

2. D. Kim, S. Ramani and J. A. Fessler, "Accelerating X-ray CT ordered subsets image reconstruction with Nesterov's first-order methods" In Proc. Intl. Mtg. on Fully 3D Image Recon. in Rad. and Nuc. Med pp. 22–5, 2013.
3. F. Durand and J. Dorsey, "Fast bilateral filtering for the display of high dynamic range images," ACM Transactions on Graphics, Vol. 21, No. 3, pp. 257–266, 2002.
4. T. Goldstein and S. Osher, "The Split Bregman Method for L1 Regularized Problems," SIAM Journal on Imaging Sciences, Vol. 2, No. 2, pp. 323–34, 2009.
5. A. Chambolle, "An algorithm for total variation minimization and applications," Journal of Matter Image and Visualization', Journal Roy Statistic Society, Vol. 20, No. 1, pp. 89–97, 2004.
6. C. Tomasi and R. Manduchi. Bilateral filtering for gray and color images. In Sixth International Conference on Computer Vision, pages 836–846, Jan 1998.
7. Z. Li, L. Yu, J. D. Trzasko, D. S. Lake, D. J. Blezek, J. G. Fletcher, C. H. McCollough and A. Manduca, "Adaptive nonlocal means filtering based on local noise level for CT denoising," International Journal of Medical Physics Research and Practice, Vol. 41, No. 1, 2014.
8. S. Mallat, "A theory for multiresolution signal decomposition: the wavelet representation," IEEE Trans. on Pattern Anal. Mach. Intell., Vol. 11, No. 7, pp. 674–693, 1989.
9. A. Fathi and A. R. Naghsh-Nilchi, "Efficient image denoising method based on a new adaptive wavelet packet thresholding function," IEEE Trans Image Process, Vol. 21, No. 9, pp. 3981–3990, 1989.
10. D. L. Donoho and I. M. Johnstone, "Ideal spatial adaptation via wavelet shrinkage," Biometrika, Vol. 81, pp. 425–455, 1994.
11. A. Borsdorf, R. Raupach, T. Flohr and J. Hornegger Tanaka, "Wavelet Based Noise Reduction in CT-Images Using Correlation Analysis," IEEE Transactions on Medical Imaging, Vol. 27, No. 12, pp. 1685–1703, 2008.
12. D. L. Donoho, "De-noising by soft-thresholding," IEEE Transactions on Information Theory, Vol. 41, No. 3, pp. 613–627. Signal Process. Vol. 90 no. 8 pp 2529–2539, 2010, 1995.
13. F. Abramovitch, T. Sapatinas, and B. W. Silverman "Wavelet thresholding via a Bayesian approach," Journal Roy Statistic Society, Vol. 60, No. 4, pp.725– 749, 1998.
14. J. Romberg, H. Choi and R. G. Baraniuk, "Bayesian wavelet domain image modeling using hidden Markov models," IEEE Transactions on Image Processing, Vol. 10, pp. 1056–1068, 2001.
15. S. G. Chang, B. Yu and M. Vetterli, "Adaptive wavelet thresholding for image denoising and compression," IEEE Trans. on Image Proc, Vol. 9, No. 9, pp. 1532–1546, 2000.
16. L. Xinhao, M. Tanaka and M. Okutomi, "Single- Image Noise Level Estimation for Blind Denoising," IEEE Transactions on Image Processing, Vol. 22, No. 12, pp. 5226–5237, 2013.
17. H. S. Bhadauria and M. L. Dewal, "Efficient Denoising Technique for CT images to Enhance Brain Hemorrhage Segmentation," International Journal of Digit Imaging, Vol. 25, No. 6, pp. 782–791, 2012.
18. P. Jain and V. Tyagi, "LAPB: Locally adaptive patch-based wavelet domain edge-preserving image denoising," Journal of Information Sciences, Vol. 294, pp. 164–181, 2015.
19. S. Sahu, A.K. Singh, S.P. Ghrera, and M. Elhoseny, "An approach for de-noising and contrast enhancement of retinal fundus image using CLAHE" Optics & Laser Technology, 2018.
20. Sahu, Sima, Harsh Vikram Singh, Basant Kumar, and Amit Kumar Singh. "Statistical modeling and Gaussianization procedure based de-speckling algorithm for retinal OCT images." Journal of Ambient Intelligence and Humanized Computing (2018): 1–14.

21. Sahu, Sima, Harsh Vikram Singh, Basant Kumar, and Amit Kumar Singh. "De-noising of ultrasound image using Bayesian approached heavy-tailed Cauchy distribution." Multimedia Tools and Applications (2017): 1–18.
22. Sahu, Sima, Harsh Vikram Singh, Basant Kumar, and Amit Kumar Singh. "A Bayesian multiresolution approach for noise removal in medical magnetic resonance images." Journal of Intelligent Systems (2018).
23. Luisier, Florian, and Thierry Blu. "SURE-LET multichannel image denoising: interscale orthonormal wavelet thresholding." Image Processing, IEEE Transactions on 17.4 (2008): 482–492.